JACS
JOURNAL OF THE AMERICAN CHEMICAL SOCIETY
pubs.acs.org/JACS
Article

Photocatalyzed Diastereoselective Isomerization of Cinnamyl Chlorides to Cyclopropanes

Bin Xu, Ludovic Troian-Gautier,* Ryan Dykstra, Robert T. Martin, Osvaldo Gutierrez,* and Uttam K. Tambar*

Cite This: J. Am. Chem. Soc. 2020, 142, 6206−6215
Read Online
ACCESS | Metrics & More | Article Recommendations | Supporting Information

ABSTRACT: Endergonic isomerizations are thermodynamically unfavored processes that are difficult to realize under thermal conditions. We report a photocatalytic and diastereoselective isomerization of acyclic cinnamyl chlorides to strained cyclopropanes. Quantum mechanical calculations (uM06-2X and DLPNO), including TD-DFT calculations, and experimental studies provide evidence for the energy transfer from an iridium photocatalyst to the allylic chloride substrate followed by C−Cl homolytic cleavage. Subsequent Cl• radical migration forms a localized triplet 1,3-diradical intermediate that, after intersystem crossing, undergoes ring-closing to form the desired product. The mild reaction conditions are compatible with a broad range of functional groups to generate chlorocyclopropanes in high yields and diastereoselectivities. A more efficient process is developed by addition of a catalytic amount of a nickel complex, and we propose a novel role for this cocatalyst to recycle an allyl chloride byproduct generated in the course of the reaction. The reaction is also shown to be stereoconvergent, as an *E*/*Z* mixture of cinnamyl chlorides furnish the *anti*-chlorocyclopropane product in high diastereoselectivity. We anticipate that the use of a visible light activated photocatalyst to transform substrates in combination with a transition metal catalyst to recycle byproducts back into the catalytic cycle will provide unique opportunities for the discovery of new reactivity.

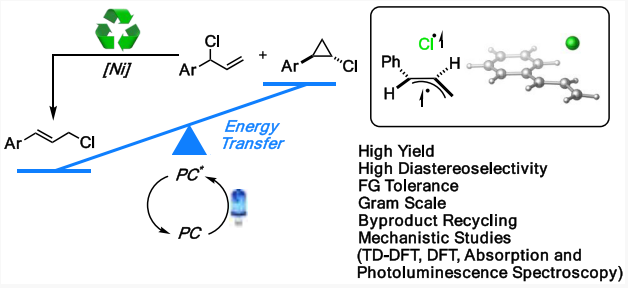

INTRODUCTION

Molecules incorporating cyclopropanes have fascinated organic chemists for decades. The cyclopropyl group is a common motif found in many pharmaceutical products and secondary metabolites.[1] This privileged functional group is employed to increase metabolic stability, enhance potency, and decrease plasma clearance in druglike molecules.[2] The strain associated with the cyclopropane ring system (approximately 27 kcal/mol), along with the electronic character of its bent carbon−carbon bonds, has been the subject of many seminal discoveries in chemical structure and bonding.[3] Moreover, the unique reactivity of cyclopropanes has been exploited for the synthesis of several distinct classes of products.[4]

Given the general intrigue and practical utility of cyclopropanes, synthetic chemists have developed elegant strategies for the assembly of these three-membered ring systems. To date, most approaches are based on the reaction of stable substrates with high energy reagents that provide the potential energy necessary for generating strained cyclopropanes (Figure 1). Popular strategies for cyclopropane synthesis include [2 + 1]-type cycloadditions between alkenes and reactive reagents, such as carbene equivalents generated from diethylzinc and dihalomethanes (Simmons−Smith reaction)[5] or metal carbenes generated from diazo compounds (Figure 1A).[6] In some

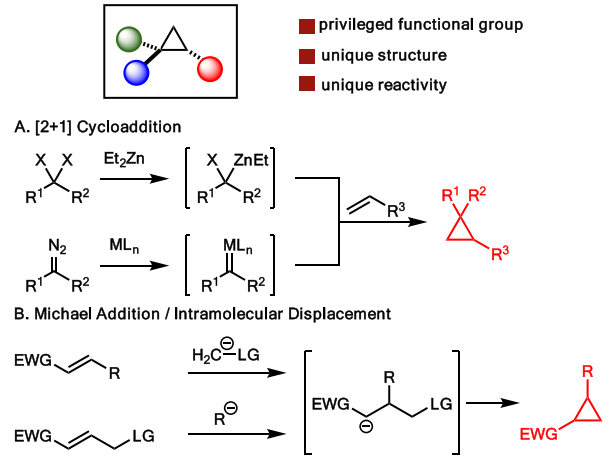

Figure 1. Classical methods to synthesize cyclopropanes.

Received: January 6, 2020
Published: March 4, 2020

https://dx.doi.org/10.1021/jacs.0c00147
J. Am. Chem. Soc. 2020, 142, 6206−6215

cases (Figure 1B), a two-step process (Michael-type or Giese addition followed by intramolecular displacement) can be employed for the cyclopropanation of activated alkenes (e.g., sulfur ylides with enones in the Corey−Chaykovsky reaction or alkyl radicals in radical-polar crossover cyclopropanations).[7] Although these routes are well-established in the literature, they are often lacking in broad functional group tolerance and operational simplicity and rarely employ mild conditions. More recently, photoreducible and photooxidizable C_1 reagents and olefins, in combination with a photoredox catalyst, have been developed by Suero,[8] Molander,[9] Aggarwal,[10] and others.[11]

We were interested in developing a different strategy to access strained cyclopropanes via the photocatalytic *unimolecular isomerization* of their low energy acyclic precursors (Figure 2A). If successful, this novel approach would be a more

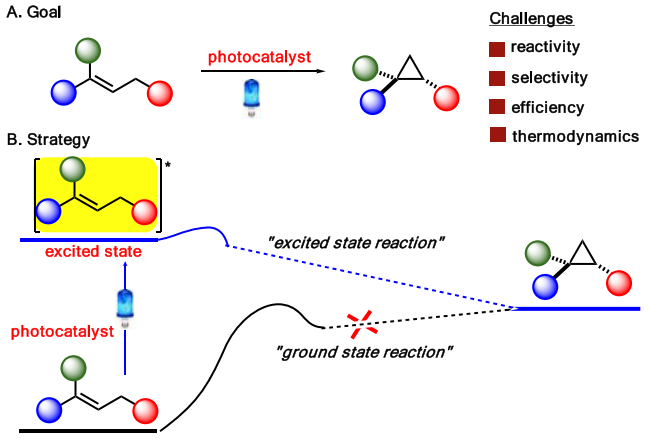

Figure 2. Energetically uphill isomerization of acyclic compounds to strained cyclopropanes.

atom-economic and direct synthesis of cyclopropanes. However, the thermal isomerization from a low energy substrate to a high energy strained product is an energetically endergonic process ($\Delta G_{rxn} > 0$) and, hence, represents an extremely challenging "*uphill*" transformation.

Photochemistry has been utilized as an alternative strategy for mediating energetically endergonic isomerizations.[12] In this context, elegant photocatalytic processes have recently been reported for the isomerization of *trans*-alkenes to *cis*-alkenes[13] and of cyclic alcohols to acyclic carbonyl compounds.[14] A selective and high-yielding photocatalytic isomerization of acyclic compounds to strained cyclopropanes is unprecedented, and it represents a unique challenge to the concept of controlling energetically endergonic isomerizations (Figure 2B). Herein, we present a photocatalytic system for the diastereoselective synthesis of *anti*-chlorocyclopropanes from their acyclic cinnamyl chloride precursors. In addition to exploring the scope and synthetic utility of this general transformation, we performed experimental and computational studies to gain insight into the overall mechanism.

RESULTS AND DISCUSSION

Allylic chlorides were selected as an initial starting point to develop an energetically endergonic isomerization of acyclic compounds to strained cyclopropanes. Early studies with this class of substrates suggested that the photochemical isomerization of allylic chlorides could furnish cyclopropane products. UV irradiation of allylic chlorides such as **1a** with organic photosensitizers led to a mixture of rearranged products, including chlorocyclopropanes **2a** and **4a** as well as acyclic allylic chloride **3a**, albeit in low yields and poor product selectivities (Figure 3).[15] Despite the potential utility of these

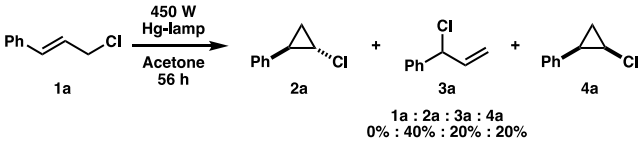

Figure 3. Early studies of photochemical isomerization of allylic chlorides.

transformations, their synthetic applicability remains severely limited and their mechanism is poorly defined. Based on these results and recent efforts on endergonic photocatalytic reactions, we hypothesized that the use of a photoredox catalyst and visible light, along with a deeper mechanistic understanding of this photochemical isomerization, could lead to a more efficient and functional group tolerant strategy for generating a broad range of strained chlorocyclopropanes.[16]

To commence our studies, we subjected cinnamyl chloride **1a** to different photocatalysts under blue LED light irradiation (Table 1). 2,4,6-Triphenylpyrylium tetrafluoroborate (**5**), a typical organophotocatalyst, did not catalyze any conversion of cinnamyl chloride **1a** (entry 1). We turned our attention to metal polypyridyl-based photocatalysts. The ruthenium-centered photocatalyst, $[Ru(bpy)_3](PF_6)_2$ (**6**), did not activate the cinnamyl chloride **1a** either (entry 2). To our delight, iridium-

Table 1. Initial Results by Testing Various Photocatalysts

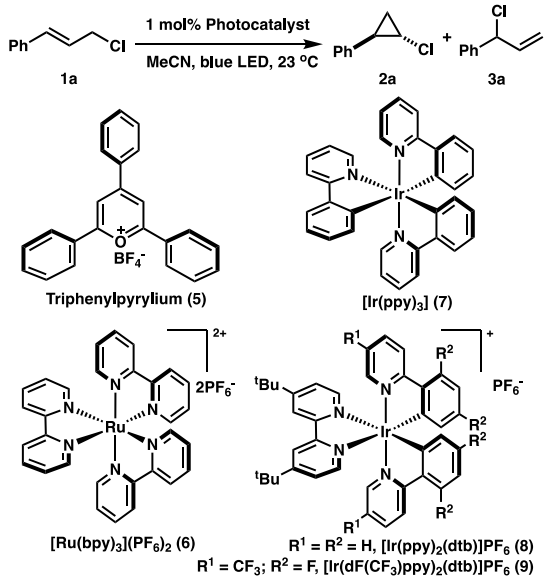

entry[a]	photocatalyst	time (h)	ratio of **1a**/**2a**/**3a**/**4a**[b] (%)
1	**5**	24	100, 0, 0, 0
2	**6**	24	100, 0, 0, 0
3	**7**	24	60, 20, 10, 0
4	**8**	16	0, 44, 46, 0
5	**9**	16	0, 48, 42, 0
6	**9**	72	0, 52, 36, 0

[a]Reaction conditions: photocatalyst (1 mol %), **1a** (0.2 mmol), MeCN (1 mL), 4 W blue LED. [b]^{1}H NMR yields based on 1,3,5-tribromobenzene as an internal standard.

https://dx.doi.org/10.1021/jacs.0c00147
J. Am. Chem. Soc. 2020, 142, 6206−6215

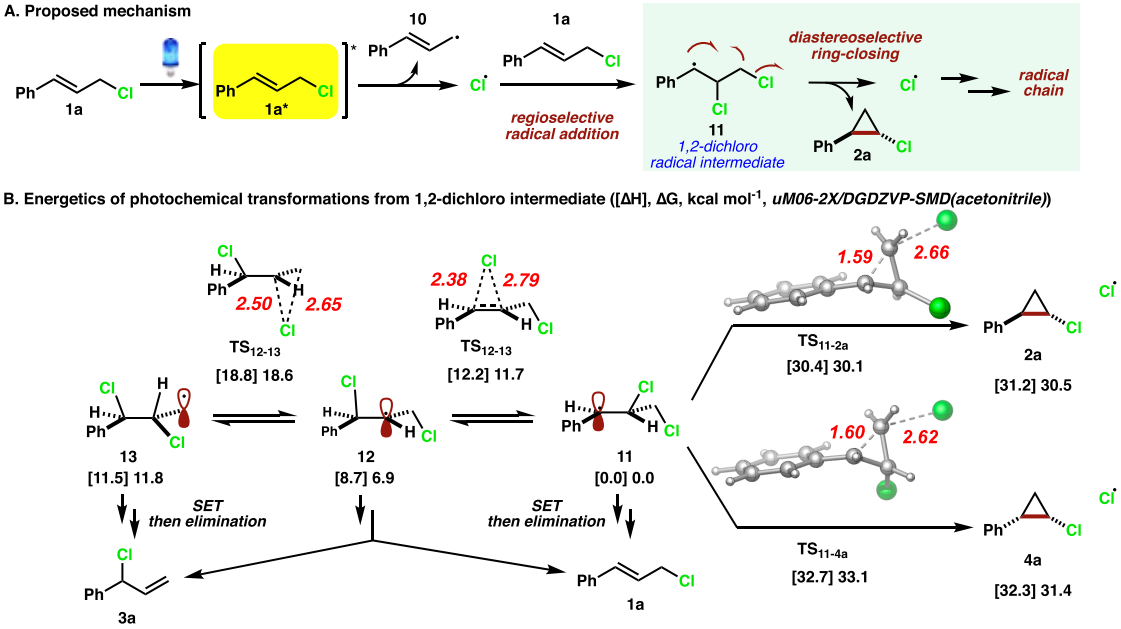

Figure 4. DFT calculations of mechanism that proceeds through dichloro radical intermediates.

centered photocatalyst $Ir(ppy)_3$ (**7**) partially converted linear substrate **1a** to the desired cyclopropane product **2a**, with a significant amount of undesired branched allylic chloride **3a** as byproduct (entry 3). Interestingly, while early examples of photochemical isomerization of allylic chlorides in the presence of UV light yielded diastereomers **2a** and **4a** in a 2:1 ratio (Figure 3),[15] under our mild visible-light mediated photocatalyzed conditions, chlorocyclopropane **2a** was formed as the only diastereomer. Additional iridium-centered photocatalysts were then examined, including $[Ir(ppy)_2(dtb)]PF_6$ (**8**) and $[Ir(dF(CF_3)ppy)_2(dtb)]PF_6$(**9**) (entries 4−6). Both of these metal polypyridyl complexes furnished full conversion of **1a** and provided a moderate yield of desired product **2a**. A significant amount of byproduct **3a** was also obtained, even if the reaction time was extended to 72 h (entry 6). Certain classes of allylic chlorides and other allylic substrates, including allylic bromides, iodides, fluorides, alcohols, and acetates, did not furnish the desired cyclopropane product under the reaction conditions (Table S4).

Previous mechanistic studies on similar systems supported triplet−triplet energy transfer leading to an excited triplet state as the first intermediate in these photosensitized isomerizations.[15] However, the nature of subsequent steps remain poorly understood (i.e., homolytic or heterolytic C−Cl bond breaking, zwitterionic or singlet/triplet diradical intermediates, radical-cage recombination/cyclization, etc.). In an effort to optimize the conversion of acyclic allylic chloride **1a** to cyclopropane **2a** and gain insights into the mechanism of formation of byproduct **3a**, we turned to quantum mechanical calculations. All structures were optimized using unrestricted DFT with M06-2X functional and a DGDZVP basis set in acetonitrile (SMD solvation model) as implemented in Gausian09.[17] To refine energetics, we performed subsequent single point calculations with a def2-TZVPP basis set (uM06-2X/def2-TZVPP-SMD(acetonitrile)//uM06-2X/DGDZVP-SMD(acetonitrile)). For comparison, we also performed single point energy calculations using DLPNO−CCSD(T) (with solvent corrections from (uM06-2X/def2-TZVPP-SMD-(acetonitrile) single point calculations) and the def2-TZVPP basis set using ORCA software version 4.1.2.[9a,18] For simplicity, only uM06-2X singlet point calculations will be discussed in the manuscript. Minimum energy crossing points were found using the MECPro version 1.0.5.[19] Structures were visualized using CYLview version 1.0.[20] See the Supporting Information for further details.

Akin to our recent calculations on photoredox cyclopropanation studies,[9a] we initially hypothesized that a photochemically generated chlorine atom could undergo regioselective Giese addition to cinnamyl chloride **1a** leading to the formation of 1,2-dichloro radical intermediate **11** (Figure 4A). In turn, equilibration to the lowest energy dichloro intermediate will be proceeded by diastereoselective ring-closing to form the desired product **2a** (Figure 4A, inset). To assess the feasibility of radical cyclization from the presumed 1,2-dichloro radical intermediate **11**, we performed quantum mechanical calculations (Figure 4B). Although calculations predict facile isomerization between 1,3- and 1,2-dichloro radical species **11**, **12**, and **13**, the barriers to undergo the desired radical cyclization from **11** leading to cyclopropane products **2a** and **4a** are >30 kcal/mol (i.e., $\mathbf{TS}_{\mathbf{11-2a}}$ and $\mathbf{TS}_{\mathbf{11-4a}}$), and the reactions are highly endergonic. Based on these results, we ruled out the formation of cyclopropane products from dichloro intermediates (**11**, **12**, and **13**). Our previously reported quantum mechanical calculations[9a] demonstrated that, under appropriate photoredox catalysis, halogen radical intermediates can undergo facile single electron transfer (SET) with the photocatalyst to form an anionic species (via a radical-polar crossover mechanism). In turn, the anionic species could then undergo facile ring-closure with concomitant release of a halide anion. However, all attempts to locate the corresponding dichloro anionic species from **11**, **12**, and **13** failed and led to direct formation of elimination products **1a** and **3a** as shown in Figure 4 (see also Figure S1A in the Supporting Information). Thus, quantum mechanical calculations ruled against formation of dichloro radical or anionic species as key intermediates in the photochemical isomerization (see the Supporting Information for further details).

https://dx.doi.org/10.1021/jacs.0c00147
J. Am. Chem. Soc. 2020, 142, 6206−6215

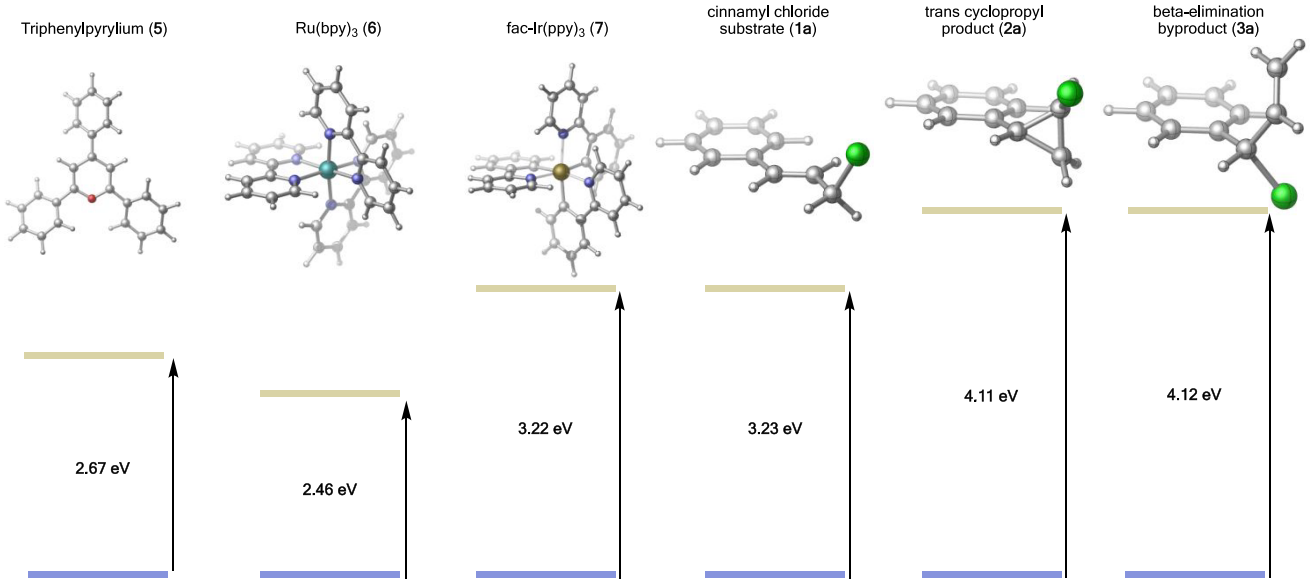

Figure 5. Lowest energy excitations to triplet states of photocatalysts and substrate (out of 10 excitations) using TD-DFT [uM062X/DGDZVP-SMD(acetonitrile)].

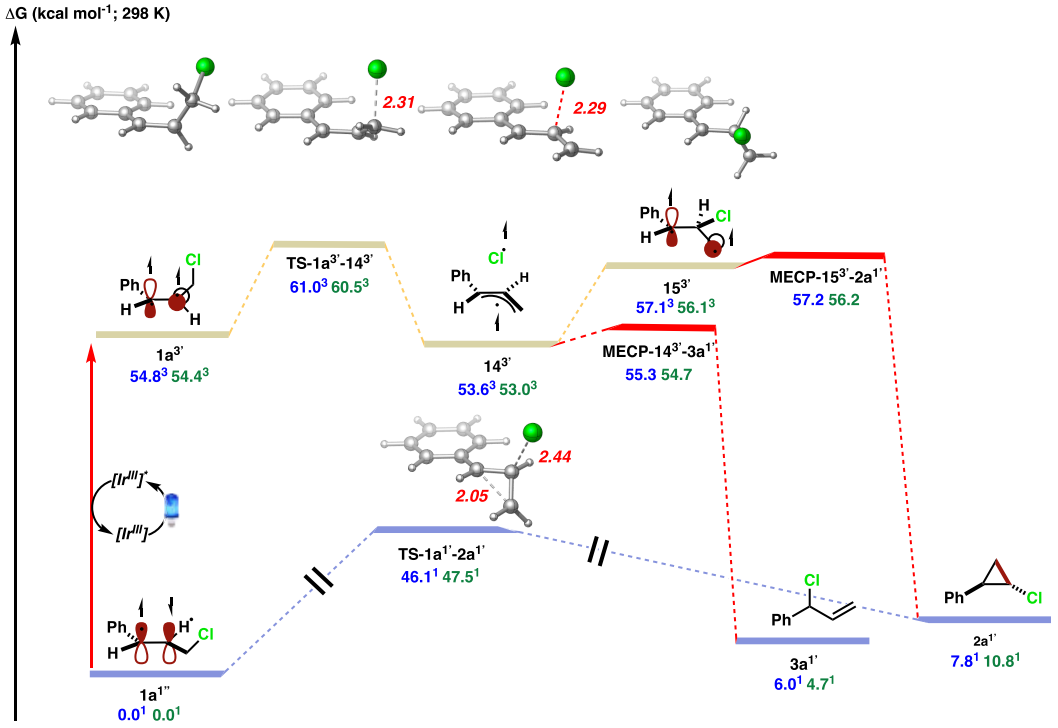

Figure 6. Energetics for photocatalytic isomerization. Free energies, in kcal/mol, are from UM06-2X/def2-TZVPP-SMD(acetonitrile) (blue) and DLPNO−CCSD(T)/def2-TZVPP-SMD(acetonitrile) (green) calculations.

Next, we focused on examining cyclopropanation via a *triplet* spin state surface. TD-DFT calculations on cinnamyl chloride **1a** revealed that the lowest lying *singlet* excitation, 4.86 eV, is inaccessible directly by blue LED irradiation, which is consistent with the experimentally determined UV/vis absorption spectrum of substrate **1a** (Figure S5).[21] We then suspected that triplet−triplet energy transfer may allow for excitation of the cinnamyl chloride to its *triplet* state.[15] As shown in Figure 5, the *triplet* excited state of cinnamyl chloride **1a** is inaccessible via ruthenium (**6**) and triphenylpyrylium (**5**) *triplet* excited states. Notably, Ir-based photocatalyst **7** has the energy requirements to promote triplet−triplet energy transfer and is thus able to activate the allylic chloride substrate. Additional TD-DFT calculations affirm that excitation of the product **2a** and byproduct **3a** is not possible under these conditions (Figure 5), making this transformation photochemically irreversible and allowing for a productive endergonic isomerization.

Assuming facile triplet−triplet energy transfer from the excited state of the photocatalyst **7** to the cinnamyl chloride $\mathbf{1a}^{1''}$, the triplet intermediate $\mathbf{1a}^{3'}$ can then undergo *homolytic* carbon-chlorine bond dissociation (via $\mathbf{TS\text{-}1a}^{3'}\mathbf{\text{-}14}^{3'}$) to form

https://dx.doi.org/10.1021/jacs.0c00147
J. Am. Chem. Soc. 2020, 142, 6206−6215

isoenergetic triplet radical pair $\mathbf{14}^{3\prime}$ with an overall barrier of only ~6 kcal/mol from $\mathbf{1a}^{3\prime}$ (Figure 6). This intermediate, albeit lower in energy, could undergo C−Cl bond formation to form 1,3-diradical triplet intermediate $\mathbf{15}^{3\prime}$ via an almost barrierless (~4.0 kcal/mol via ultrafine scan) Cl radical recombination (Figure S3B). We located a *triplet* transition state ring-closing from $\mathbf{15}^{3\prime}$ to form the desired cyclopropane in the *triplet spin state* (not shown), but this process was ruled out because it has an insurmountable kinetic barrier (>40 kcal/mol) and it is endergonic by more than 35 kcal/mol from $\mathbf{15}^{3\prime}$ (Figure S3). Importantly, from the two *triplet* diradical intermediates $\mathbf{14}^{3\prime}$ and $\mathbf{15}^{3\prime}$ we located the corresponding minimum energy crossing points (**MECP-**$\mathbf{14}^{3\prime}$**-**$\mathbf{3a}^{1\prime}$ and **MECP-**$\mathbf{15}^{3\prime}$**-**$\mathbf{2a}^{1\prime}$) that will form the experimentally observed branched allylic chloride and cyclopropane products $\mathbf{3a}^{1\prime}$ and $\mathbf{2a}^{1\prime}$, respectively, after intersystem crossing. All singlet MECP had a single imaginary frequency which, upon visualization, represented the desired motions that lead to products $\mathbf{3a}^{1\prime}$ and $\mathbf{2a}^{1\prime}$. Triplet MECP did not give imaginary frequencies, providing additional support that intersystem crossing to the singlet potential energy surface leads to the observed products. Notably, the barriers for these two minimum energy crossing points differ by only 1.9 kcal/mol, which is consistent with the formation of both products (entries 5 and 6, Table 1). Further, consistent with our initial hypothesis, these two products *are thermally endergonic* in energy compared to the substrate by ~6−8 kcal/mol. Overall, since the rearranged products $\mathbf{3a}^{1\prime}$ and $\mathbf{2a}^{1\prime}$ are higher in energy than the linear allylic chloride and the energy to undergo triplet−triplet energy transfer is much higher (4.11 and 4.12 eV; Figure 5), our DFT calculations suggest that this process is a result of a photochemical transformation rather than a photoinduced chain reaction. Finally, we also located the thermal concerted 1,2-sigmatropic shift/ring-closing transition state (**TS-**$\mathbf{1a}^{1\prime}$**-**$\mathbf{2a}^{1\prime}$) that will lead to product $\mathbf{2a}^{1\prime}$, which has a barrier of ~46 kcal/mol. However, this pathway was ruled out based on unfavorable *ground state* thermodynamics and kinetics.

To improve the efficiency of the photocatalyzed cyclopropanation, we hypothesized that a cocatalyst could be introduced to the reaction to *recycle* branched allylic chloride *byproduct* **3a** back into the catalytic cycle. One potential strategy would be to isomerize byproduct **3a** back to substrate **1a** with a cocatalyst that can generate metal-allyl complex **16**, such as $Pd_2(dba)_3$, $[Ir(COD)Cl]_2$, or $Ni(COD)_2$ (Table 2).[22] The use of dual catalyst systems based on photocatalysts and transition metal complexes is an emerging area of research, with several proposed roles of the transition metal complexes in light mediated processes.[23,24] In our cyclopropanation system, palladium, iridium, and nickel catalysts depressed the generation of byproduct **3a** and increased the yield of desired product **2a** (entries 1−3). Among these cocatalysts, $Ni(COD)_2$ provided the most satisfying results, including full conversion of cinnamyl chloride **1a**, total depression of branched allylic chloride **3a**, and highest yield of cyclopropane **2a** (76%, entry 3). To further improve the yield of cyclopropanation, we screened a variety of ligands for the Ni(0) cocatalyst. The coordinating ability of phosphine ligand **17** was too strong to fully isomerize **3a** (entry 4). Compared to bipyridine **18** (entry 5), bisoxazole **19** (entry 6) provided higher reactivity and yield of the desired product (86%). To ensure the full coordination and solvation of $Ni(COD)_2$/ligand complex, 12 mol % **19** was used, which resulted in 92% isolated yield of cyclopropane **2a** (entry 7).

Table 2. Optimization of Dual Catalyst System

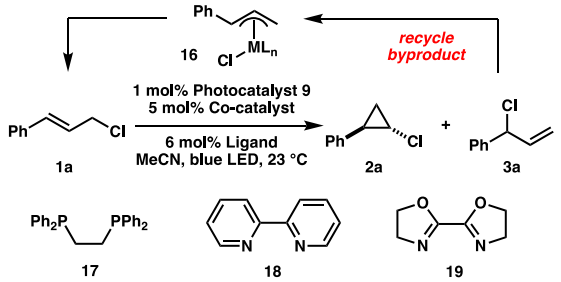

entry[a]	co-catalyst	ligand	time (h)	ratio of **1a**/**2a**/**3a**[b] (%)
1	$Pd_2(dba)_3$	none	16	16:64:0
2	$[Ir(COD)Cl]_2$	none	16	8:58:14
3	$Ni(COD)_2$	none	16	0:76:0
4	$Ni(COD)_2$	17	24	0:70:12
5	$Ni(COD)_2$	18	24	0:84:0
6	$Ni(COD)_2$	19	12	0:86:0
7[c]	$Ni(COD)_2$	19	4	0:92:0

[a]Reaction conditions: photocatalyst (1 mol %), cocatalyst (5 mol %), ligand (6 mol %), **1a** (0.2 mmol), MeCN (1 mL), 4 W blue LED. [b]^{1}H NMR yields. [c]12 mol % **19** was used.

With the optimal reaction conditions in hand, we evaluated the scope of this photocatalyzed *anti*-cyclopropanation reaction with various substituted acyclic cinnamyl chlorides **1** (Table 3). The reaction exhibited great tolerance to aromatic systems with a broad range of substituents. On the *para*-position, electron-donating groups (MeO, **2b**), alkyl substitution (Me, **2c**), aromatic rings (Ph, **2d**), halogens (F, Cl, Br; **2e**−**g**), and electron-withdrawing groups (CF_3, CO_2Me, C(=O)Me; **2h**−**j**) all provided the desired cyclopropanation products with high *anti*-selectivity (>95:5) and yields (up to 92%). Similar functional group compatibility was exhibited among the substituents on the *meta*- and *ortho*-positions (**2k**−**n**). Multisubstituted (**2o**) and fused aromatic rings (**2p** and **2q**) also afforded satisfying results. To our delight, this reaction showed tolerance to various heterocycles (**2r**−**v**), such as 1,3-benzodioxole, benzofuran, benzothiophene, indole, and pyridine. 1,1-Diaryl-substituted allylic chlorides were also examined. The corresponding cyclopropane products were obtained with high yields (**2w** and **2x**).

Further experiments were carried out to explore the synthetic potential of this photocatalyzed cyclopropanation reaction (Figure 7). First, this transformation was easily performed on gram-scale (Figure 7A). Starting from 10 mmol of commercially available cinnamyl chloride **1a**, 1.32 g of product **3a** were obtained in 87% yield with high *anti*-selectivity under mild reaction conditions. In addition, substrate **1d** furnished cyclopropane product **2d** in 94% yield. We then investigated the transformation of the C−Cl bond of chlorocyclopropane **2d** (Figure 7B). By using an in situ generated lithium morpholin-4-ide, the C−Cl bond was efficiently transformed to a C−N bond without breaking the cyclopropyl ring. Interestingly, amino-cyclopropane product **20** was obtained in 86% yield with high retention of stereochemistry, which was confirmed by X-ray crystallography.

We carried out a series of control experiments to gain insight into the mechanism of dual nickel/photocatalyzed cyclopropanation (Figure 8). First, a mixture of allylic chlorides (*Z*)-**1a**, (*E*)-**1a**, and **3a** cleanly furnished *anti*-cyclopropane **2a** with similarly high diastereoselectivity (eq 1), which suggests that

https://dx.doi.org/10.1021/jacs.0c00147
J. Am. Chem. Soc. 2020, 142, 6206−6215

Table 3. Substrate Scope[a]

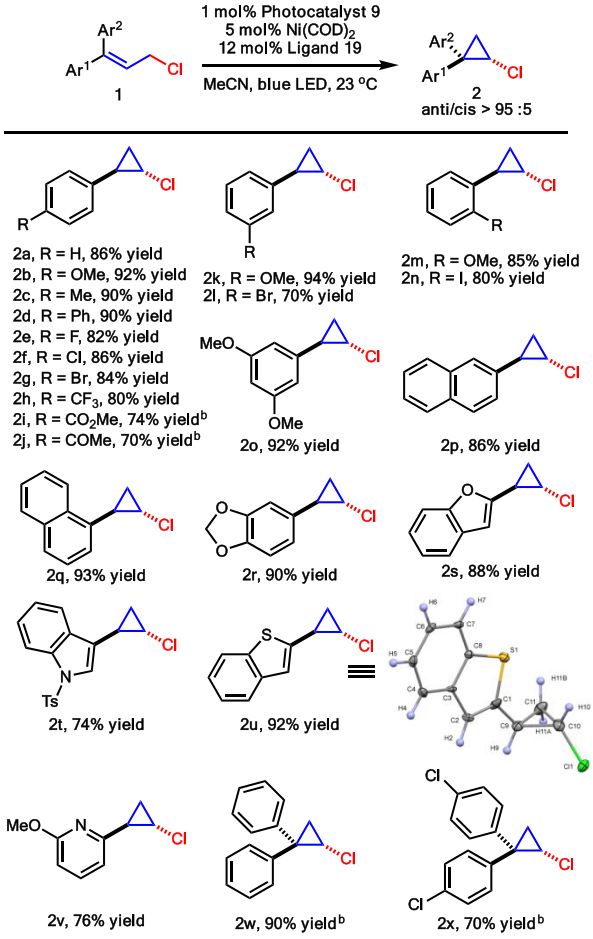

[a]Reaction conditions: photocatalyst (1 mol %), cocatalyst (5 mol %), ligand (12 mol %), **1a** (0.2 mmol), MeCN (1 mL), 4 W blue LED, 4 h, isolated yields. [b]48 h.

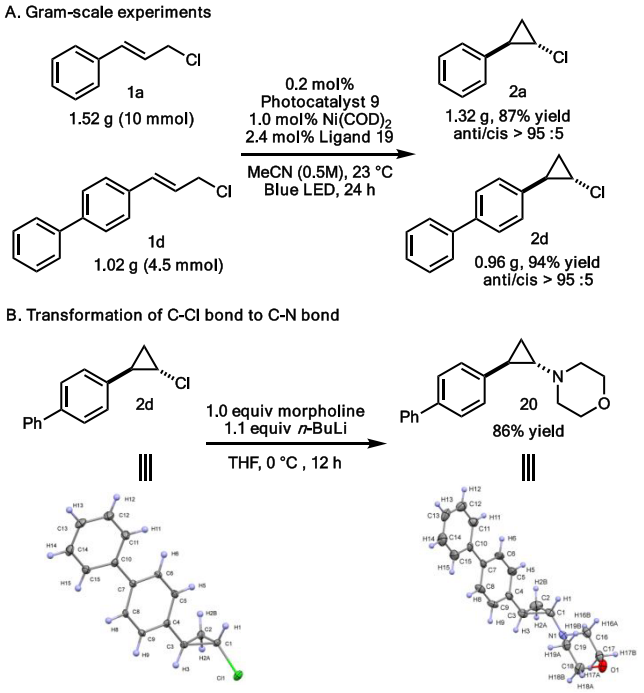

Figure 7. Synthetic utility of cyclopropanation.

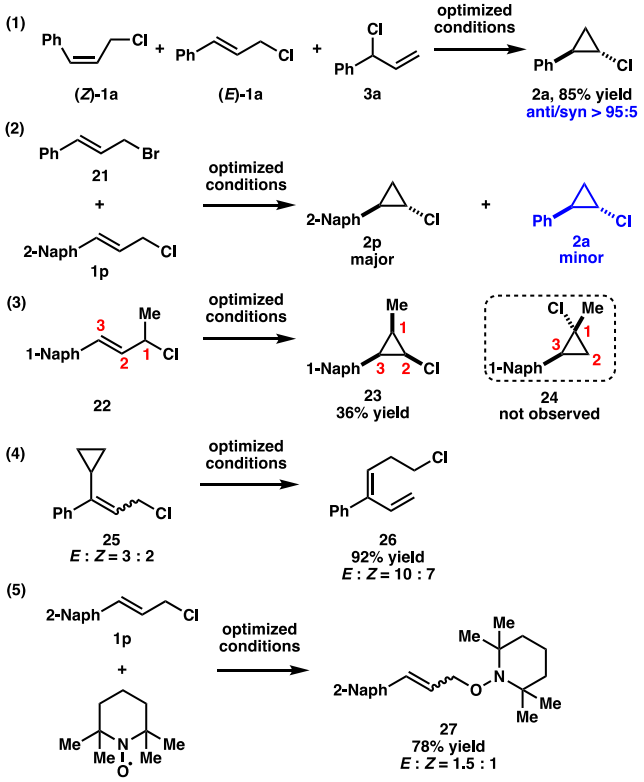

Figure 8. Mechanistic control experiments.

the mechanism involves a common intermediate that can be accessed by either linear *Z*- or *E*-allylic chloride substrates as well as branched allylic chloride byproduct **3a**. This observation represents a practical advantage to the method, as a mixture of alkene isomers of the starting material leads to the *anti*-chlorocyclopropane product **2a** through a stereoconvergent mechanism. In addition, under the optimal reaction conditions, cinnamyl bromide did not provide any cyclopropanation product. In a crossover experiment of cinnamyl bromide and 2-naphthyl substituted cinnamyl chloride, the crossover product **2a** was observed (eq 2). In line with prior computational work, this experiment implies dissociation of the C−Cl bond and bimolecular recombination during the reaction process. Interestingly, by using compound **22** as substrate, cyclopropane **23** was obtained instead of the expected cyclopropane **24** (eq 3), which is consistent with Cl migration during the reaction. A radical clock experiment with substrate **25** (eq 4) and radical-trapping experiment with TEMPO (eq 5) both support the involvement of free radical intermediates in the cyclopropanation mechanism.

Steady-state and time-resolved absorption and photoluminescence spectroscopies were used to seek additional mechanistic information on the role of the iridium photoredox catalyst. The iridium photosensitizer **9** exhibits properties that are typical of compounds with low-lying metal-to-ligand charge transfer (^{3}MLCT) excited states (Figure S6).[25] Room temperature photoluminescence centered at 470 nm was observed with an excited-state lifetime of 2.26 ± 0.20 μs. Both the steady-state as well as the time-resolved photoluminescence were efficiently quenched by various cinnamyl chloride derivatives used in the photocatalytic reactions. The quenching data was well described by the Stern−Volmer model that

https://dx.doi.org/10.1021/jacs.0c00147
J. Am. Chem. Soc. 2020, 142, 6206−6215

provided quenching rate constants, k_q that ranged from 0.47 × 10^9 M^{-1} s^{-1} (**1p**) to 3.06 × 10^9 M^{-1} s^{-1} (**1i**) (Figure 9 and

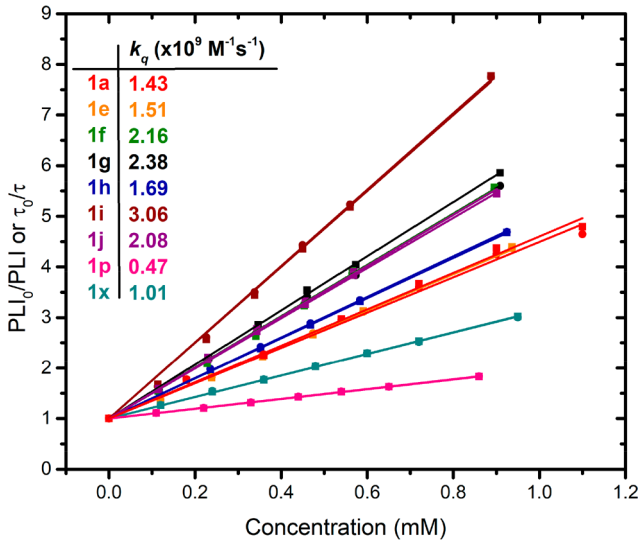

Figure 9. Stern–Volmer plots determined by steady-state (solid squares) and time-resolved (solid circles) photoluminescence for the indicated cinnamyl chloride derivatives. The quenching rate constants (k_q (× 10^9 M^{-1} s^{-1})) are indicated for each cinnamyl chloride derivative.

Figures S7–S15). Stern–Volmer plots using ratios of the steady-state (PLI_0/PLI) or time-resolved (τ_0/τ) photoluminescence were linear and coincident under the conditions used.[26] This observation ruled out *static quenching* through the formation of a ground-state adduct but rather indicated that the excited-state quenching mechanism was solely *dynamic*, i.e., that the excited-state iridium photosensitizer and the cinnamyl chloride derivative must diffuse to form an encounter complex leading to excited-state reactivity. Control Stern–Volmer experiments with (*Z*)-**1a** and **2a** were nonlinear with concentration, an observation most consistent with the formation of a less emissive adduct (Figures S16 and S17). At low concentration, the Stern–Volmer slope for excited-state quenching by (*Z*)-**1a** was slightly steeper than with the corresponding (*E*)-**1a** isomer.

Excited-state mechanistic investigations were performed using nanosecond transient absorption spectroscopy with pulsed 420 nm light excitation. First, key spectra such as the excited-state absorption spectra as well as the one-electron reduced and one-electron oxidized absorption spectra of **9** were determined (Figure 10 and Figures S18–S19).[27] These spectra are of paramount importance as they inform on the oxidation state of the iridium photosensitizer during photoredox catalysis. The excited-state absorption spectrum (blue) was characterized by an increased ΔAbs between 440 and 550 nm with a maximum centered at 480 nm. The monoreduced species exhibited a maximum at 530 nm (orange), whereas the singly oxidized species exhibited weak absorption features between 440 and 550 nm as well as above 750 nm (green). Interestingly, nanosecond transient absorption spectroscopy performed in the presence of cinnamyl chlorides **1a** or **1i** led to a drastic excited-state quenching, with an excited-state lifetime that decreased from 2.32 μs to ~10 ns (Figure 11A and Figure S20). This confirmed the excited-state quenching data quantified by Stern–Volmer experiments but did not provide

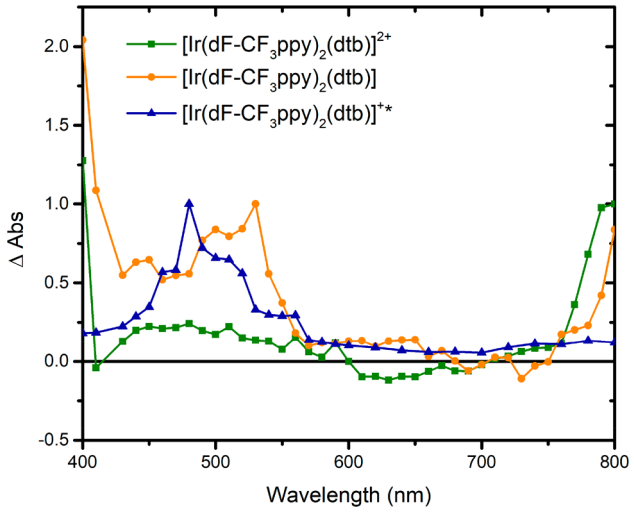

Figure 10. Absorption spectra of the oxidized [Ir(dF-CF_3 ppy)$_2$(dtb)]$^{2+}$ (green), reduced [Ir(dF-CF_3 ppy)$_2$(dtb)] (orange), and excited state [Ir(dF-CF_3 ppy)$_2$(dtb)]$^{+*}$ (blue) obtained by transient absorption spectroscopy in argon purged acetonitrile at room temperature (see the Supporting Information for additional experimental details).

evidence for the products of the quenching reactions. Had oxidative or reductive quenching of the excited state occurred in the presence of cinnamyl chlorides with cage escape yields greater than 5%, the Ir complex would have reported on the redox chemistry, contrary to what was observed. The inability to observe redox products implies either electron transfer with rapid recombination or energy transfer. Note that the photoinduced *trans–cis* isomerization of cinnamic acid derivatives with an iridium photosensitizer was recently reported to occur via triplet–triplet energy transfer.[28]

The excited-state reactivity of photocatalyst **9** with a cinnamyl amine **28** was investigated to distinguish between electron transfer and energy transfer (Figure 11B). This cinnamyl amine derivative was suspected to undergo facile electron transfer with photoredox catalysts. A quenching rate constant (k_q = 7.23 × 10^9 M^{-1} s^{-1}) was determined by Stern–Volmer analysis. Furthermore, nanosecond transient absorption spectroscopy provided undisputable evidence for electron transfer between photocatalyst **9** and cinnamyl amine **28**, with a spectral signature corresponding to both the oxidized amine and the monoreduced iridium sensitizer. Hence, the lack of spectroscopic signature observed for cinnamyl chloride **1a** or **1i** in the presence of photoexcited catalyst **9** is more consistent with an excited-state quenching mechanism that involves *energy transfer* from the excited-state Ir* to cinnamyl chloride derivatives.

On the basis of these experimental investigations and DFT calculations, we propose the mechanism depicted in Figure 12. Cinnamyl chloride **1a** is activated to the excited state **1a*** after energy transfer from irradiated Ir(III) photocatalyst **9***. Subsequently, a triplet-allyl-pair (**14**) containing chlorine radical is formed from the excited complex **1a***. There are two pathways for intermediate **14**. One path involves a direct intersystem crossing, which provides the undesired branched byproduct **3a**. The other path proceeds through triplet-β-Cl intermediate **15**, which then provides the desired cyclopropanation product **2a** after an intersystem crossing. We propose that byproduct **3a** can be recycled into the catalytic

https://dx.doi.org/10.1021/jacs.0c00147
J. Am. Chem. Soc. 2020, 142, 6206–6215

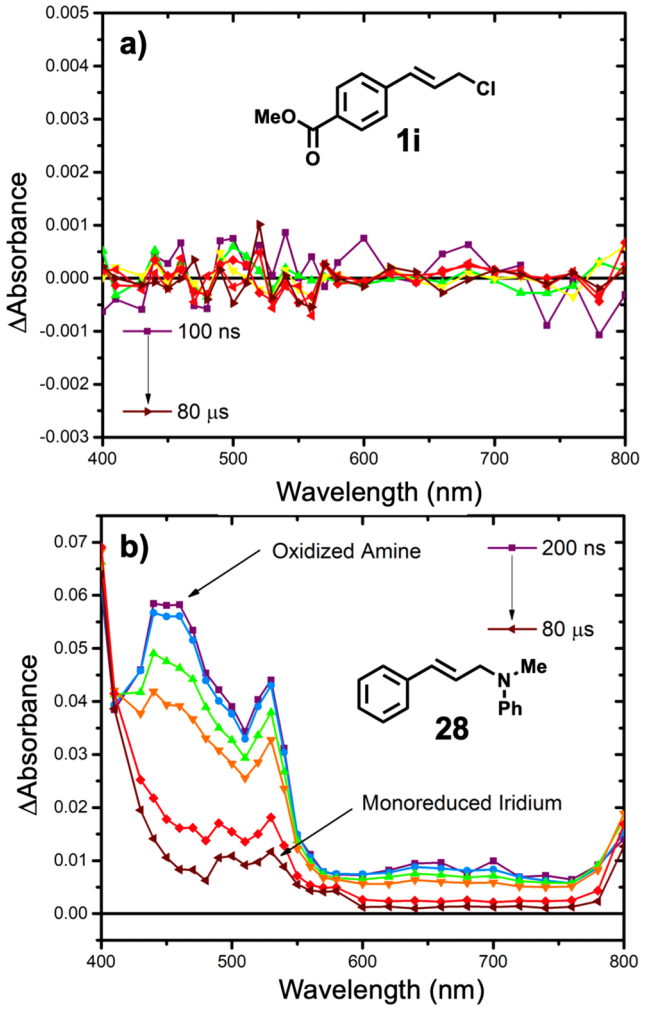

Figure 11. Pulsed 420 nm (2 mJ/Pulse) transient absorption spectroscopy of an argon-purged acetonitrile solution containing $[Ir(dF\text{-}CF_3\ ppy)_2(dtb)]^+$ and the cinnamyl derivatives **1i** and **28** (see the Supporting Information for additional experimental details).

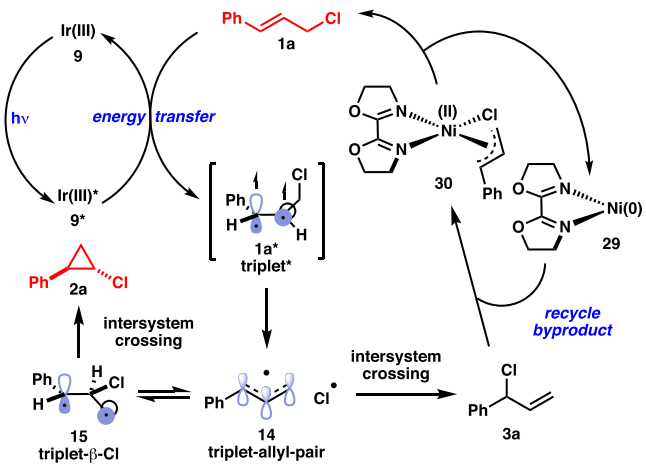

Figure 12. Proposed mechanism.

cycle via oxidative addition with Ni(0) complex **29** to form nickel allyl complex **30**, which improves the overall efficiency of the photocatalytic process. At this time, we cannot rule out the possibility that cinnamyl chloride **1a** undergoes an oxidative addition with nickel catalyst **29** to form allyl-Ni(II) complex **30**, which is then activated to the excited state **30*** via energy transfer from irritated Ir(III) photocatalyst **9***.[29] We are currently conducting mechanistic studies to examine the role of photoexcited nickel–allyl complexes.

CONCLUSION

In summary, we have developed a dual catalyst system for the efficient photocatalytic isomerization of acyclic cinnamyl chlorides that is highly diastereoselective for the formation of *anti*-chlorocyclopropanes. We provide experimental and computational evidence for the energy transfer from an iridium photocatalyst to the allylic chloride substrates, followed by a cycloisomerization to the strained cyclopropane products. The reaction demonstrates broad functional group compatibility, which can be attributed to the mildness of activation with visible light. Computational studies provided insight into the mechanism of the reaction and guided the development of a more efficient process by addition of a nickel cocatalyst. We propose a novel role for the nickel catalyst to recycle a byproduct generated in the course of the reaction. We anticipate that the use of a visible light activated photocatalyst to transform substrates in combination with a transition metal catalyst to recycle byproducts back into the catalytic cycle will provide unique opportunities for the discovery of new reactivity.

ASSOCIATED CONTENT

Supporting Information

The Supporting Information is available free of charge at https://pubs.acs.org/doi/10.1021/jacs.0c00147.

X-ray data for compound **2d** (CIF)
X-ray data for compound **2u** (CIF)
X-ray data for compound **20** (CIF)
Experimental details, characterization data, spectral data, and computational results (PDF)

AUTHOR INFORMATION

Corresponding Authors

Ludovic Troian-Gautier – *Laboratoire de Chimie Organique, Université libre de Bruxelles (ULB), 1050 Brussels, Belgium;* orcid.org/0000-0002-7690-1361; Email: ludovic.troian.gautier@ulb.ac.be

Osvaldo Gutierrez – *Department of Chemistry and Biochemistry, University of Maryland, College Park, Maryland 20742, United States;* orcid.org/0000-0001-8151-7519; Email: ogs@umd.edu

Uttam K. Tambar – *Department of Biochemistry, The University of Texas Southwestern Medical Center, Dallas, Texas 75390-9038, United States;* orcid.org/0000-0001-5659-5355; Email: uttam.tambar@utsouthwestern.edu

Authors

Bin Xu – *Department of Biochemistry, The University of Texas Southwestern Medical Center, Dallas, Texas 75390-9038, United States*

Ryan Dykstra – *Department of Chemistry and Biochemistry, University of Maryland, College Park, Maryland 20742, United States*

Robert T. Martin – *Department of Chemistry and Biochemistry, University of Maryland, College Park, Maryland 20742, United States*

Complete contact information is available at:

https://dx.doi.org/10.1021/jacs.0c00147
J. Am. Chem. Soc. 2020, 142, 6206–6215

https://pubs.acs.org/10.1021/jacs.0c00147

Author Contributions

The manuscript was written through contributions of all authors. All authors have given approval to the final version of the manuscript.

Notes

The authors declare no competing financial interest.

■ ACKNOWLEDGMENTS

O.G., R.D., and R.M. are grateful for financial support by the NSF (CAREER 1751568). O.G. is grateful to the University of Maryland College Park for start-up funds and computational resources from UMD Deepthought2 and MARCC/BlueCrab HPC clusters and XSEDE (CHE160082 and CHE160053). Financial support was provided to U.K.T. and B.X. by the W. W. Caruth, Jr. Endowed Scholarship, Welch Foundation (I-1748), National Institutes of Health (R01GM102604), American Chemical Society Petroleum Research Fund (59177-ND1), Teva Pharmaceuticals Marc A. Goshko Memorial Grant (60011-TEV), and Sloan Research Fellowship. L.T.-G. is a Postdoctoral researcher of the Fonds de la Recherche Scientifique-FNRS. L.T.-G. acknowledges Gerald J. Meyer for granting access to his equipment to complete the time-resolved experiments. We acknowledge Dr. Vincent Lynch (Manager of the X-ray Diffraction Lab at UT Austin) for the X-ray structural analysis.

■ REFERENCES

(1) (a) McGrath, N. A.; Brichacek, M.; Njardarson, J. T. A Graphical Journey of Innovative Organic Architectures That Have Improved Our Lives. *J. Chem. Educ.* **2010**, *87*, 1348−1349. (b) Wessjohann, L. A.; Brandt, W.; Thiemann, T. Biosynthesis and Metabolism of Cyclopropane Rings in Natural Compounds. *Chem. Rev.* **2003**, *103*, 1625−1648.

(2) (a) Talele, T. T. The"Cyclopropyl Fragment" is a Versatile Player that Frequently Appears in Preclinical/Clinical Drug Molecules. *J. Med. Chem.* **2016**, *59*, 8712−8756. (b) Chen, D. Y.-K.; Pouwer, R. H.; Richard, J.-A. Recent advances in the total synthesis of cyclopropane-containing natural products. *Chem. Soc. Rev.* **2012**, *41*, 4631−4642.

(3) (a) Dill, J. D.; Greenberg, A.; Liebman, J. F. Substituent effects on strain energies. *J. Am. Chem. Soc.* **1979**, *101*, 6814−6826. (b) de Meijere, A. Bonding Properties of Cyclopropane and Their Chemical Consequences. *Angew. Chem., Int. Ed. Engl.* **1979**, *18*, 809−886.

(4) (a) Wong, H. N. C.; Hon, M.-Y.; Tse, C.-W.; Yip, Y.-C.; Tanko, J.; Hudlicky, T. Use of Cyclopropanes and Their Derivatives in Organic Synthesis. *Chem. Rev.* **1989**, *89*, 165−198. (b) Carbocyclic Three-Membered Ring Compounds: Cyclopropanes, Transformations. *Houblen-Weyl Methods of Organic Chemistry*; Thieme: Stuttgart, Germany, 1997; Vol. *E17c*. (c) Carson, C. A.; Kerr, M. A. Heterocycles from Cyclopropanes: Applications in Natural Product Synthesis. *Chem. Soc. Rev.* **2009**, *38*, 3051−3060. (d) Ebner, C.; Carreira, E. M. Cyclopropanation Strategies in Recent Total Syntheses. *Chem. Rev.* **2017**, *117*, 11651−11679.

(5) (a) Simmons, H. E.; Smith, R. D. A New Synthesis of Cyclopropanes from Olefins. *J. Am. Chem. Soc.* **1958**, *80*, 5323−5324. (b) Simmons, H. E.; Smith, R. D. A New Synthesis of Cyclopropanes. *J. Am. Chem. Soc.* **1959**, *81*, 4256−4264. (c) Simmons, H. E.; Cairns, T. L.; Vladuchick, S. A.; Hoiness, C. M. Cyclopropanes from Unsaturated Compounds, Methylene Iodide, and Zinc-Copper Couple. *Org. React.* **1973**, *20*, 1−131.

(6) (a) Doyle, M. P.; McKervey, M. A.; Ye, T. *Modern Catalytic Methods for Organic Synthesis with Diazo Compounds: From Cyclopropanes to Ylides*; Wiley-Interscience: New York, 1998. (b) Davies, H. M. L. Dirhodium Tetra(*N*-arylsulfonylprolinates) as Chiral Catalysts For Asymmetric Transformations of Vinyl- and Aryldiazoacetates. *Eur. J. Org. Chem.* **1999**, *1999*, 2459−2469.

(7) Patai, S.; Rappoport, Z. *The Chemistry of the Cyclopropyl Group*; Wiley & Sons: New York, 1987; Chapter 9.

(8) (a) del Hoyo, A. M.; Herraiz, A. G.; Suero, M. G. A Stereoconvergent Cyclopropanation Reaction of Styrenes. *Angew. Chem., Int. Ed.* **2017**, *56*, 1610−1613. (b) del Hoyo, A. M.; Suero, M. G. Photoredox-Catalyzed Cyclopropanation of Michael Acceptors. *Eur. J. Org. Chem.* **2017**, *2017*, 2122−2125. (c) Herraiz, A. G.; Suero, M. G. New Alkene Cyclopropanation Reactions Enabled by Photoredox Catalysis via Radical Carbenoids. *Synthesis* **2019**, *51*, 2821−2828. (d) Herraiz, A. G.; Suero, M. G. A transition-metal-free & diazo-free styrene cyclopropanation. *Chem. Sci.* **2019**, *10*, 9374−9379.

(9) (a) Phelan, J. P.; Lang, S. B.; Compton, J. S.; Kelly, C. B.; Dykstra, R.; Gutierrez, O.; Molander, G. A. Redox-Neutral Photocatalytic Cyclopropanation via Radical/Polar Crossover. *J. Am. Chem. Soc.* **2018**, *140*, 8037−8047. (b) Milligan, J. A.; Phelan, J. P.; Polites, C. C.; Kelly, C. B.; Molander, G. A. Radical/Polar Annulation Reactions (RPARs) Enable the Modular Construction of Cyclopropanes. *Org. Lett.* **2018**, *20*, 6840−6844. (c) Milligan, J. A.; Burns, K. L.; Le, A. V.; Polites, V. C.; Wang, Z.-J.; Molander, G. A.; Kelly, C. B. Radical-Polar Crossover Annulation: A Platform for Accessing Polycyclic Cyclopropanes. *Adv. Synth. Catal.* **2020**, *362*, 242−247.

(10) Shu, C.; Mega, R. S.; Andreassen, B. J.; Noble, A.; Aggarwal, V. K. Synthesis of Functionalized Cyclopropanes from Carboxylic Acids by a Radical Addition-Polar Cyclization Cascade. *Angew. Chem., Int. Ed.* **2018**, *57*, 15430−15434.

(11) (a) Guo, T.; Zhang, L.; Liu, X.; Fang, Y.; Jin, X.; Yang, Y.; Li, Y.; Chen, B.; Ouyang, M. Visible-Light-Promoted Redox-Neutral Cyclopropanation Reactions of α-Substituted Vinylphosphonates and Other Michael Acceptors with Chloromethyl Silicate as Methylene Transfer Reagent. *Adv. Synth. Catal.* **2018**, *360*, 4459−4463. (b) Li, P.; Zhao, J.; Shi, L.; Wang, J.; Shi, X.; Li, F. Iodine-catalyzed diazo activation to access radical reactivity. *Nat. Commun.* **2018**, *9*, 1972. (c) Sayes, M.; Benoit, G.; Charette, A. B. Borocyclopropanation of Styrenes Mediated by UV-light Under Continuous Flow Conditions. *Angew. Chem., Int. Ed.* **2018**, *57*, 13514−13518. (d) Luo, W.; Yang, Y.; Fang, Y.; Zhang, X.; Jin, X.; Zhao, G.; Zhang, L.; Li, Y.; Zhou, W.; Xia, T.; Chen, B. Photoredox-Catalyzed Cyclopropanation of 1,1-Disubstituted Alkenes via Radical-Polar Crossover Process. *Adv. Synth. Catal.* **2019**, *361*, 4215−4221. (e) Ohtani, T.; Tsuchiya, Y.; Uraguchi, D.; Ooi, T. Photocatalytic borylcyclopropanation of α-boryl styrenes. *Org. Chem. Front.* **2019**, *6*, 1734−1737.

(12) De Mayo, P., Ed. *Organic Chemistry, Vol. 42: Rearrangements in Ground and Excited States*; Academic Press, 1980; Vol. *1*−*3*.

(13) (a) Singh, K.; Staig, S. J.; Weaver, J. D. Facile Synthesis of Z-Alkenes via Uphill Catalysis. *J. Am. Chem. Soc.* **2014**, *136*, 5275−5278. (b) Zheng, C.; Wan-Min, C.; Li, H.-L.; Na, R.-S.; Shang, R. Cis-Selective Decarboxylative Alkenylation of Aliphatic Carboxylic Acids with Vinyl Arenes Enabled by Photoredox/Palladium/Uphill Triple. *Org. Lett.* **2018**, *20*, 2559−2563. (c) Metternich, J. B.; Gilmour, R. A Bio-Inspired, Catalytic E - Z Isomerization of Activated Olefins. *J. Am. Chem. Soc.* **2015**, *137*, 11254−11257. (d) Metternich, J. B.; Artiukhin, D. G.; Holland, M. C.; von Bremen-Kühne, M.; Neugebauer, J.; Gilmour, R. Photocatalytic E - Z Isomerization of Polarized Alkenes Inspired by the Visual Cycle: Mechanistic Dichotomy and Origin of Selectivity. *J. Org. Chem.* **2017**, *82*, 9955−9977. (e) Pearson, C. M.; Snaddon, T. N. Alkene Photo-Isomerization Inspired by Vision. *ACS Cent. Sci.* **2017**, *3*, 922−924. (f) Litman, Z. C.; Wang, Y.; Zhao, H.; Hartwig, J. F. Cooperative asymmetric reactions combining photocatalysis and enzymatic catalysis. *Nature* **2018**, *560*, 355−359. (g) Molloy, J. J.; Metternich, J. B.; Daniliuc, C. G.; Watson, A. J. B.; Gilmour, R. Contra-Thermodynamic, Photocatalytic E-Z Isomerization of Styrenyl Boron Species: Vectors to Facilitate Exploration of Two-Dimensional Chemical Space. *Angew. Chem., Int. Ed.* **2018**, *57*, 3168−3172. (h) Faßbender, S. I.; Molloy, J. J.; Mück-Lichtenfeld, C.; Gilmour, R. Geometric E-Z Isomerisation of Alkenyl Silanes by Selective Energy Transfer Catalysis: Stereodivergent Synthesis of

Triarylethylenes via a Formal anti-Metallometallation. *Angew. Chem., Int. Ed.* **2019**, *58*, 18619−18626. (i) Livingstone, K.; Tenberge, M.; Pape, F.; Daniliuc, C. G.; Jamieson, C.; Gilmour, R. Photocatalytic E - Z Isomerization of β-Ionyl Derivatives. *Org. Lett.* **2019**, *21*, 9677−9680. (j) Meng, Q.-Y.; Schirmer, T. E.; Katou, K.; König, B. Controllable Isomerization of Alkenes by Dual Visible-Light-Cobalt Catalysis. *Angew. Chem., Int. Ed.* **2019**, *58*, 5723−5728. (k) Naskar, S.; Roy Chowdhury, S.; Mondal, S.; Maiti, D. K.; Mishra, S.; Das, I. Visible-Light-Activated Divergent Reactivity of Dienones: Dimerization in Neat Conditions and Regioselective E to Z Isomerization in the Solvent. *Org. Lett.* **2019**, *21*, 1578−1582.

(14) Ota, E.; Wang, H.; Frye, N. L.; Knowles, R. R. A Redox Strategy for Light-Driven, Out-of-Equilibrium Isomerizations and Application to Catalytic C-C Bond Cleavage Reactions. *J. Am. Chem. Soc.* **2019**, *141*, 1457−1462.

(15) (a) Cristol, S. J.; Lee, G. A. Photochemical Transformations. V. Allylic Rearrangements and Rearrangement of Allylic Halides to Cyclopropyl Halides. *J. Am. Chem. Soc.* **1969**, *91*, 7554−7555. (b) Cristol, S. J.; Lee, G. A.; Noreen, A. L. Photochemical transformations. VIII. Photosensitized Rearrangements of Some Acyclic Allylic Halides. *J. Am. Chem. Soc.* **1973**, *95*, 7067−7074. (c) Cristol, S. J.; Micheli, R. P. Photochemical Transformations. XI. Photochemical and Thermal Rearrangements of Some beta-Substituted Allylic Systems. *J. Org. Chem.* **1975**, *40*, 667−672. (d) Cristol, S. J.; Daughenbaugh, R. J.; Opitz, R. J. Photochemical Transformations. 19. Photosensitized Reactions of beta-Methylallyl Chloride. *J. Am. Chem. Soc.* **1977**, *99*, 6347−6353.

(16) For recent reviews of photoredox catalysis, see: (a) Narayanam, J. M. R.; Stephenson, C. R. J. Visible light photoredox catalysis: applications in organic synthesis. *Chem. Soc. Rev.* **2011**, *40*, 102−113. (b) Yoon, T. P.; Ischay, M. A.; Du, J. Visible light photocatalysis as a greener approach to photochemical synthesis. *Nat. Chem.* **2010**, *2*, 527−532. (c) Prier, C. K.; Rankic, D. A.; MacMillan, D. W. C. Visible Light Photoredox Catalysis with Transition Metal Complexes: Applications in Organic Synthesis. *Chem. Rev.* **2013**, *113*, 5322−5363. (d) Arias-Rotondo, D. M.; McCusker, J. K. The photophysics of photoredox catalysis: a roadmap for catalyst design. *Chem. Soc. Rev.* **2016**, *45*, 5803−5820. (e) Douglas, J. J.; Sevrin, M. J.; Stephenson, C. R. J. Visible Light Photocatalysis: Applications and New Disconnections in the Synthesis of Pharmaceutical Agents. *Org. Process Res. Dev.* **2016**, *20*, 1134−1147.

(17) Zhao, Y.; Truhlar, D. G. The M06 suite of density functionals for main group thermochemistry, thermochemical kinetics, noncovalent interactions, excited states, and transition elements: two new functionals and systematic testing of four M06-class functionals and 12 other function. *Theor. Chem. Acc.* **2008**, *120*, 215−241.

(18) (a) Neese, F. The ORCA program system. Wiley Interdiscip. *Wiley Interdiscip. Rev.: Comput. Mol. Sci.* **2012**, *2*, 73−78. (b) Riplinger, C.; Sandhoefer, B.; Hansen, A.; Neese, F. Natural triple excitations in local coupled cluster calculations with pair natural orbitals. *J. Chem. Phys.* **2013**, *139*, 134101.

(19) Snyder, J. D.; Hamill, L.-A.; Faleumu, K. E.; Ess, D. H. *MECPro Version 1.0.5: Minimum Energy Crossing Program*, 2019.

(20) Legault, C. Y. *CYLview*, rev 1.0b; Université de Sherbrooke, 2009; http://www.cylview.org.

(21) Andrews, L. J.; Linden, S. L. Allylidene Halides. II. The Structure and Reactivity of Cinnamal Chloride. *J. Am. Chem. Soc.* **1947**, *69*, 2091−2094.

(22) For reviews, see: (a) Kazmaier, U. Palladium catalyzed allylic alkylations of nonstabilized enolates. *Curr. Org. Chem.* **2003**, *7*, 317−328. (b) Miyabe, H.; Takemoto, Y. Regio- and stereocontrolled palladium- or iridium-catalyzed allylation. *Synlett* **2005**, 1641−1655. (c) Nishibayashi, Y.; Uemura, S. In *C-C bond formation (part 2) by substitution reactions: allylic alkylation*; Elsevier, Ltd., 2007; pp 75−122. (d) Falciola, C. A.; Alexakis, A. Copper-catalyzed asymmetric allylic alkylation. *Eur. J. Org. Chem.* **2008**, *2008* (22), 3765−3780. (e) Hong, A. Y.; Stoltz, B. M. The Construction of All-Carbon Quaternary Stereocenters by Use of Pd-Catalyzed Asymmetric Allylic Alkylation Reactions in Total Synthesis. *Eur. J. Org. Chem.* **2013**, *2013*, 2745−2759. (f) Trost, B. M. Metal catalyzed allylic alkylation: its development in the Trost laboratories. *Tetrahedron* **2015**, *71*, 5708−5733. (g) Hethcox, J. C.; Shockley, S. E.; Stoltz, B. M. Iridium-Catalyzed Diastereo-, Enantio-, and Regioselective Allylic Alkylation with Prochiral Enolates. *ACS Catal.* **2016**, *6*, 6207−6213. (h) Hornillos, V.; Gualtierotti, J.-B.; Feringa, B. L. Asymmetric allylic substitutions using organometallic reagents. *Top. Organomet. Chem.* **2016**, *58*, 1−39. (i) Trost, B. M.; Schultz, J. E. Palladium-Catalyzed Asymmetric Allylic Alkylation Strategies for the Synthesis of Acyclic Tetrasubstituted Stereocenters. *Synthesis* **2019**, *51*, 1−30. (j) Cheng, Q.; Tu, H.-F.; Zheng, C.; Qu, J.-P.; Helmchen, G.; You, S.-L. Iridium-Catalyzed Asymmetric Allylic Substitution Reactions. *Chem. Rev.* **2019**, *119*, 1855−1969.

(23) For recent reviews, see: (a) Twilton, J.; Le, C.; Zhang, P.; Shaw, M. H.; Evans, R. W.; MacMillan, D. W. C. The Merger of Transition Metal and Photocatalysis. *Nat. Rev. Chem.* **2017**, *1*, 0052. (b) Skubi, K. L.; Blum, T. R.; Yoon, T. P. Dual Catalysis Strategies in Photochemical Synthesis. *Chem. Rev.* **2016**, *116*, 10035−10074.

(24) For a recent study reported from our laboratory, see: Xu, B.; Tambar, U. K. Remote Allylation of Unactivated C(sp3)-H Bonds Triggered by Photogenerated Amidyl Radicals. *ACS Catal.* **2019**, *9*, 4627−4631.

(25) (a) Bevernaegie, R.; Marcélis, L.; Laramée-Milette, B.; De Winter, J.; Robeyns, K.; Gerbaux, P.; Hanan, G. S.; Elias, B. Trifluoromethyl-Substituted Iridium(III) Complexes: From Photophysics to Photooxidation of a Biological Target. *Inorg. Chem.* **2018**, *57*, 1356−1367. (b) Deaton, J. C.; Castellano, F. N. Archetypal Iridium(III) Compounds for Optoelectronic and Photonic Applications. In *Iridium(III) in Optoelectronic and Photonics Applications*; Wiley: 2017. (c) Bevernaegie, R.; Marcélis, L.; Moreno-Betancourt, A.; Laramée-Milette, B.; Hanan, G. S.; Loiseau, F.; Sliwa, M.; Elias, B. Ultrafast charge transfer excited state dynamics in trifluoromethyl-substituted iridium(iii) complexes. *Phys. Chem. Chem. Phys.* **2018**, *20*, 27256−27260.

(26) (a) Lakowicz, J. R. *Principles of Fluorescence Spectroscopy*; Springer: New York, 2006. (b) Troian-Gautier, L.; Turlington, M. D.; Wehlin, S. A. M.; Maurer, A. B.; Brady, M. D.; Swords, W. B.; Meyer, G. J. Halide Photoredox Chemistry. *Chem. Rev.* **2019**, *119*, 4628−4683.

(27) DiMarco, B. N.; Troian-Gautier, L.; Sampaio, R. N.; Meyer, G. J. Dye-sensitized electron transfer from TiO2 to oxidized triphenylamines that follows first-order kinetics. *Chem. Sci.* **2018**, *9*, 940−949.

(28) Kerzig, C.; Wenger, O. S. Reactivity control of a photocatalytic system by changing the light intensity. *Chem. Sci.* **2019**, *10*, 11023−29.

(29) For related studies of photoexcited nickel complexes, see: (a) Heitz, D. R.; Tellis, J. C.; Molander, G. A. Photochemical Nickel-Catalyzed C-H Arylation: Synthetic Scope and Mechanistic Investigations. *J. Am. Chem. Soc.* **2016**, *138*, 12715−12718. (b) Welin, E. R.; Le, C.; Arias-Rotondo, D. M.; McCusker, J. K.; MacMillan, D. W. C. Photosensitized, Energy Transfer-Mediated Organometallic Catalysis through Electronically Excited Nickel(II). *Science* **2017**, *355*, 380−385. (c) Kim, T.; McCarver, S. J.; Lee, C.; MacMillan, D. W. C. Sulfonamidation of Aryl and Heteroaryl Halides through Photosensitized Nickel Catalysis. *Angew. Chem., Int. Ed.* **2018**, *57*, 3488−3492.

https://dx.doi.org/10.1021/jacs.0c00147
J. Am. Chem. Soc. 2020, 142, 6206−6215